

A SMALL-ANGLE X-RAY SCATTERING STATION AT BEIJING SYNCHROTRON RADIATION FACILITY

Zhihong Li, Zhonghua Wu, Guang Mo, Xueqing Xing, and Peng Liu

Beijing Synchrotron Radiation Facility, Institute of High Energy Physics,
Chinese Academy of Sciences, Beijing, China

□ This article presents the development and current state of a small-angle X-ray scattering station at beamline 1W2A of the Beijing Synchrotron Radiation Facility, China. The source of the beamline is introduced from a 14-pole wiggler. A triangular bending Si(111) crystal is used to horizontally focus the beam and provide a monochromatic X-ray beam (8.052 keV). A bending cylindrical mirror coated with rhodium downstream from the monochromator is used to vertically focus the beam. The X-ray beam is focused on the detector which is fixed at 30 m from the source. The focused beam size (full width at half maximum) is $1.4 \times 0.2 \text{ mm}^2$ (horizontal \times vertical) with a flux of 5.5×10^{11} phs/s at 2.5 GeV and 250 mA. Besides the routine mode of small-angle X-ray scattering, the combination of small- and wide-angle X-ray scattering, grazing incidence small-angle X-ray scattering, and time-resolved small-angle X-ray scattering in sub-second level are also available for the users. Dependent on the measurement requirements, several detectors can be chosen for the collection of scattering signals. Furthermore, multiple sample environments, including temperature, stress-strain, and liquid sampling are available for in situ measurements. In a typical camera length of 1.5 m, the small-angle X-ray scattering resolution is about 115 nm. The steady operation of the small-angle X-ray scattering station at Beijing Synchrotron Radiation Facility not only provides the small-angle X-ray scattering beam time for users, but also promotes the development and application of these techniques in China.

Keywords BSRF, SAXS, station

INTRODUCTION

Small-angle X-ray scattering (SAXS) is a powerful tool to study nanoscale structures in various materials.^[1] Especially, due to the use of a synchrotron radiation (SR) source, small-angle X-ray scattering techniques have experienced a rapid development period in the past decades. At present, small-angle X-ray scattering facilities have become one of the

Address correspondence to Zhonghua Wu, Beijing Synchrotron Radiation Facility, Institute of High Energy Physics, Chinese Academy of Sciences, 19B Yuquan Road, Beijing 100049, China. E-mail: wuzh@ihep.ac.cn

main experimental stations at most synchrotron research centers.^[2] In addition, many new scattering techniques have been developed based on small-angle X-ray scattering beamlines or instruments that include the wide-angle X-ray scattering technique (WAXS), the combined small- and wide-angle X-ray scattering technique (SAXS/WAXS), grazing incidence small-angle X-ray scattering technique (GISAXS), anomalous small-angle X-ray scattering technique (ASAXS), time-resolved small-angle X-ray scattering technique (t-SAXS), and ultra-small angle X-ray scattering technique (USAXS). These techniques are useful to provide structural information of matter. The community of small-angle X-ray scattering facility users is rapidly growing in China during this period. However, the existing small-angle X-ray scattering facility did not satisfy the needs of experiment time. In this case, a new dedicated small-angle X-ray scattering station based on beamline 1W2A was proposed and constructed at Beijing Synchrotron Radiation Facility (BSRF) in Beijing at the end of 2007. In addition to the anomalous small-angle X-ray scattering and the ultra-small angle X-ray scattering techniques, this station supports all the other techniques mentioned above. This station has been open to users for about five years. A detailed description about its current status, such as configuration and application, will be given in this article.

BEAMLINE

At Beijing Synchrotron Radiation Facility, the small-angle X-ray scattering beamline 1W2A and the protein crystallography beamline 1W2B share the same synchrotron radiation source from a 14-pole wiggler (1W2) at the storage ring of Beijing Electron Positron Collider (BEPC).^[3] At the front-end of 1W2, a water-cooling carbon filter is used to reduce the thermal powder density from the white synchrotron radiation beam. After the carbon filter, a triangular bending Si(111) crystal located at 20 m from the 1W2 source is used to separate horizontally the beam into 5-mrad 1W2A and 1.5-mrad 1W2B. Beamline 1W2A is deflected from the beam 1W2 at an angle of 28.42°. Simultaneously, the triangular bending Si(111) crystal is also used to monochromatize the white beam for beamline 1W2A and horizontally focus the beam, providing a monochromatic X-ray beam with energy fixed at 8.052 keV and energy resolution of about 7.0×10^{-4} ($\Delta E/E$). The rest of the white beam without deflection goes directly to the beamline 1W2B downstream where independent monochromator and focusing mirror are used to optimize the beamline 1W2B for protein crystallography. Downstream of the beamline 1W2A, a bending cylindrical mirror coated with rhodium is placed 2.1 m away from the triangular bending Si(111) monochromator. This mirror is used to vertically focus the X-ray beam.

To have high resolution of the reciprocal space, both horizontal and vertical focusing spots are optimized to focus onto the small-angle X-ray scattering detector, which is installed at the end of beamline 1W2A and is 30 m far away from the source. The final monochromatic X-ray beam has a flux of about 5×10^{11} photons/s and a divergence of 2.4 mrad (horizontal) \times 0.5 mrad (vertical) at sample position. Depending on the stability of storage ring and optical elements on the beamline, this beam position stability is evaluated to be better than 3% RMS (root-mean-square) within 5 s and better than 10% RMS within one hour. The focused X-ray spot size (full width at half maximum, FWHM) is about 1.4 mm (horizontal) \times 0.2 mm (vertical). For the convenience of the experimental-mode switch and the length adjustment of the small-angle X-ray scattering camera, a beryllium window is used to segregate the downstream low-vacuum small-angle X-ray scattering camera from the upstream high-vacuum optical elements. Figure 1 shows a schematic map of beamline 1W2A at the Beijing Synchrotron Radiation Facility. The corresponding beamline parameters are summarized in Table 1.

In order to depress the harmful scattering background and improve the small-angle X-ray scattering data quality, an effective and reliable collimation system is very important for a small-angle X-ray scattering beamline.^[4] In the beamline 1W2A, a three-slit system is used to collimate the incident X-ray beam. The first and the second slits are located downstream from the monochromator with a distance of 0.9 m and 4.8 m, respectively. The first and the second slits are used to define the beam size and divergence. The third slit is a guard slit, which is placed in front of and as close as possible to the sample. A scatterless slit (VSLT100) from Forvis Technologies^[5] is equipped as the guard slit. In order to protect the detector from the radiation damage of the direct beam, several beam-stops with different size and shape (circular and rectangle) are available. In addition, different lengths of low-vacuum pipes are available to change the length of small-angle X-ray scattering camera.

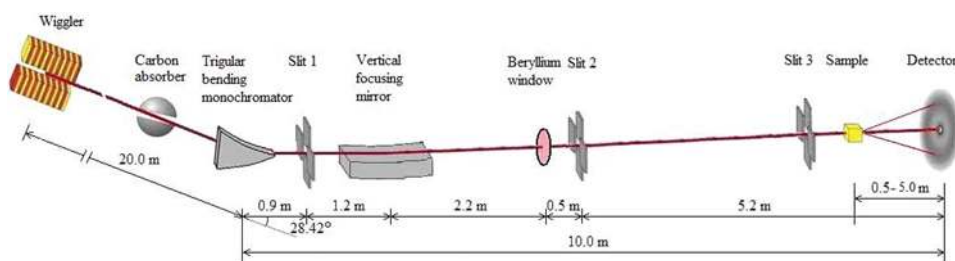


FIGURE 1 Schematic map of beamline 1W2A and the small-angle X-ray scattering station at Beijing Synchrotron Radiation Facility. (color figure available online.)

TABLE 1 Parameters of Beamline 1W2A and the Small-angle X-ray Scattering Station at Beijing Synchrotron Radiation Facility

Parameters	Value
Storage ring energy	2.5 GeV
Source	14-pole wiggler
Monochromator	Horizontally focusing triangular Si(111) crystal
X-ray energy	8.052 keV
Energy resolution	7.0×10^{-4} ($\Delta E/E$)
Mirror	Vertical focusing rhodium-coating Si mirror
Flux at sample	5.5×10^{11} photons/s
Sample to detector maximum distance	5.0 m
Beam size (FWHM) at detector	About $1.4 \times 0.2 \text{ mm}^2$ ($H \times V$)
Observable d -spacing @ 1.5 m camera length	1.5 ~ 115 nm
Measurement mode	Small- and/or wide-angle X-ray scattering, grazing incidence small-angle X-ray scattering, and time-resolved small-angle X-ray scattering

EXPERIMENTAL STATION

Detectors

There are four types of detectors available at the 1W2A small-angle X-ray scattering station now. They are a two-dimensional Mar165 CCD,^[6] a one-dimensional linear (L-150) gas detector,^[7] one-dimensional curved (C-200-90) gas detectors,^[7] and a two-dimensional Pilatus 1M-F detector (installed recently).^[8] According to the experimental requirements, users can choose the proper detectors to collect the small- and/or wide-angle X-ray scattering patterns.^[9–14] The performance parameters of the detectors are compared in Table 2. Generally, the CCD detector is capable for most samples especially for that with moderate- and high-scattering capability. The frame-shift mode of the CCD detector makes it possible to collect the scattering patterns in millisecond level.^[6] The gas detectors seem to be beneficial to weak scattering samples. Although the gas detector is capable of sub-millisecond time resolution, its lower count rate often limits its application at synchrotron radiation source. The Pilatus detector is the best choice for the time-resolved small-angle X-ray scattering measurements in millisecond level.

Sample Environments

Several ancillary components are available as shown in Figure 2, including a stress-strain equipment ($0 \sim 2000 \text{ N}$), a temperature and stress-strain equipment ($0 \sim 200 \text{ N}$, $-196^\circ\text{C} \sim +350^\circ\text{C}$), a variable temperature equipment for liquids (-30°C to $+90^\circ\text{C}$), a heater (from room temperature to 1100°C), a bottom heater (RT to $+300^\circ\text{C}$), and a stop-flow device

TABLE 2 Performance Parameters of the Detectors at the 1W2A Small-angle X-ray Scattering Station of Beijing Synchrotron Radiation Facility

Model	Mar165 CCD	L-150	C-200-90	Pilatus 1 M-F
Vender	Mar USA	D2L, France	D2L, France	DECTRIS, Switzerland
Type	Charge coupled device	Position sensitive gas filled detector	Position sensitive gas filled detector	hybrid pixel detector
Active area	Diameter 165 mm	$150 \times 8 \text{ mm}^2$	$314 \times 8 \text{ mm}^2$ (Radius 200 mm, angular range 90°)	$169 \times 179 \text{ mm}^2$
Spatial resolution	100 μm	200 μm	150 μm	172 μm
Global count rate	Unlimited during exposure	10^5 cps	10^5 cps	2×10^6
Read-out time	3.5 s	μs	μs	2.3 ms
Read-out noise	13e^-	0	0	0
Dynamic range	10^4	10^6	10^6	10^6
Application	small- or wide-angle X-ray scattering	small- or wide-angle X-ray scattering	wide-angle X-ray scattering	small-angle X-ray scattering

($\Delta t = 0.25 \text{ ms}$, -10 to $+80^\circ\text{C}$). These devices are used to provide different sample environments^[10,15–18] for *in situ* measurements.

Experimental Modes

In order to satisfy the different requirements from different samples and users, the small-angle X-ray scattering station was designed to include multiple experimental modes. Small- or/and wide-angle X-ray scattering,^[9–11,14,19,20] grazing incidence small-angle X-ray scattering,^[18,21] and time-resolved small-angle X-ray scattering^[11,13] are available.

The basic experimental mode is routine small-angle X-ray scattering or wide-angle X-ray scattering. The detectable region of scattering angle (2θ) or scattering vector ($q = 4\pi\sin\theta/\lambda$) is mainly determined by the length of the small-angle X-ray scattering camera for a fixed detector. For a typical small-angle X-ray scattering measurement, the incident X-ray wavelength is fixed at 1.54 \AA , the beam-stop size is chosen as 4 mm , and a CCD with diameter of 165 mm is chosen as the detector. When the small-angle X-ray scattering camera is 1.5 m in length, the detectable scattering vector (q) is from $0.0054\text{--}0.43 \text{ \AA}^{-1}$, which corresponds to an observable correlation distances ($d\text{-spacing}$) from $1.5\text{--}115 \text{ nm}$. Usually, the longer of the small-angle X-ray scattering camera, the smaller of the detectable minimum q value (q_{min}) or the larger of the detectable maximum scatterer size (d_{max}). The maximum length of the small-angle X-ray scattering camera is about 5 m at this station.

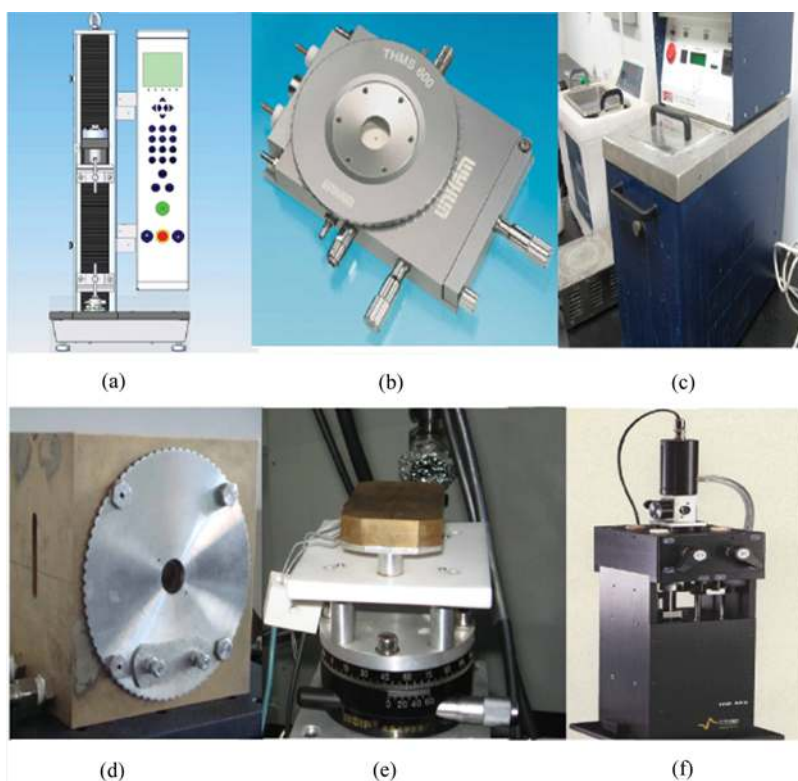


FIGURE 2 Ancillary equipments providing different environments for sample at the 1W2A small-angle X-ray scattering station. (a) a stress-strain equipment (0–2000 N); (b) a temperature and stress-strain equipment (0–200 N, -196°C to $+350^{\circ}\text{C}$); (c) a liquid variable temperature device (-30°C to $+90^{\circ}\text{C}$); (d) heater (from room temperature to 1100°C); (e) a sample bottom heater (RT to $+300^{\circ}\text{C}$); and (f) a stop-flow equipment ($\Delta t = 0.25$ ms, -10 to $+80^{\circ}\text{C}$). (color figure available online.)

The combination of small-angle and wide-angle X-ray scattering measurements are available in this station. The small-angle and wide-angle X-ray scattering signals are collected simultaneously with two detectors. The detectable angle (or scattering vector) range for small-angle scattering and wide-angle scattering depends on the sample to detector distance, the active area of detector, and the tilt angle of detector. When the two-dimensional Mar165 CCD detector together with a one-dimensional gas detector or the two-dimensional Pilatus detector are used for the combining small-angle and wide-angle X-ray scattering measurements, a transistor-transistor logic (TTL) pulse from the CCD is used as the trigger to drive another detector working simultaneously. When the two-dimensional Pilatus 1M-F detector and a one-dimensional gas detector are used for measurements, the former is triggered by the TTL signal from the latter. When two one-dimensional gas detectors are used for small-angle and wide-angle X-ray scattering

simultaneous measurements, they share the same electronics control system. The small-angle and wide-angle X-ray scattering curves recorded with both detectors are displayed in the same graphical interface. As an example, Figure 3 shows the combination of small-angle and wide-angle X-ray scattering patterns of certain carbon fiber sample collected with two one-dimensional gas detectors.^[14] Three obvious diffraction peaks are observed from the wide-angle X-ray scattering pattern within a detectable scattering vector range from 10–49 nm⁻¹. A decay scattering intensity with the scattering vector q is also shown in the pattern. In principle, the wide-angle X-ray scattering pattern can be used to determine the crystalline structure in the carbon fibers, and the size and distribution of the micropores in the carbon fibers can also be extracted from the small-angle X-ray Scattering pattern.

Grazing incidence small-angle X-ray scattering is often used to study thin film with a substrate; therefore a reflective geometry is used in these measurements. To control and adjust accurately the X-ray incidence angle, a 5-freedom sample stage is used to hold the sample, which includes the rotation around three orthogonal axes and the translation along the vertical and horizontal axes. The three-rotation precision is about 0.001° and the two-translation precision is about 5 μm. A bottom-heating stage can be used to heat the sample from room temperature to 350°C. A typical grazing incidence small-angle X-ray scattering pattern recorded with Mar165

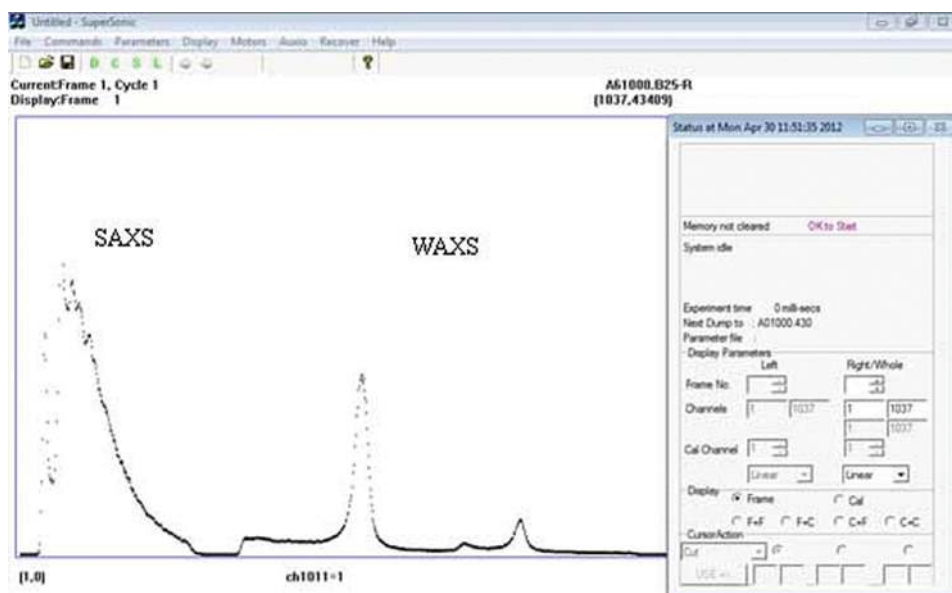


FIGURE 3 Combining small-angle and wide-angle X-ray scattering patterns of certain carbon fibers recorded by two one-dimensional gas detectors at the 1W2A small-angle X-ray scattering station.^[14] (color figure available online.)

CCD is shown in Figure 4, which is from a multilayer mesoporous silica membrane. The grazing incident angle of X-ray was set to 0.17° . From Figure 4, it can be seen that the scattering pattern is not isotropic although the three intense spots tend to locate at a circle. Roughly, the q_z direction (i.e., the vertical direction of Figure 4) corresponds to a smaller dimension, but the q_y direction (i.e., the horizontal direction of Figure 4) is related with a bigger dimension. Detailed structural information about the multilayers can be obtained by simulation of the grazing incidence small-angle X-ray scattering pattern.

Depending on the response and readout time of a detector, the practicable incident X-ray intensity, and the sample environment, time-resolved small-angle X-ray scattering measurements can be performed in time intervals from millisecond to minutes. This is helpful for *in situ* study on the sample structure change and its mechanism.

Computer Control and Data Processing Software

The computer control system of the small-angle X-ray scattering station can be classified as two parts. One is for alignment of optical components and sample environments; another is for control of data collection, storage, output, and processing.

The control software is written in the Labview language with a graphical interface. Usually, the scattering data collection is computer-controlled with the corresponding detector control software from the vendors. The incident X-ray intensity is monitored by an ion chamber in front of the sample. The transmitted X-ray intensity is recorded by an ion chamber

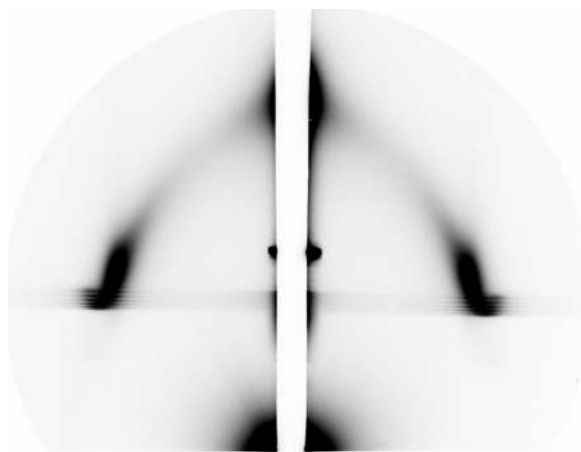


FIGURE 4 Grazing incidence small-angle X-ray scattering pattern of a multilayer mesoporous silica membrane recorded with Mar 165 CCD detector at the 1W2A small-angle X-ray scattering station.

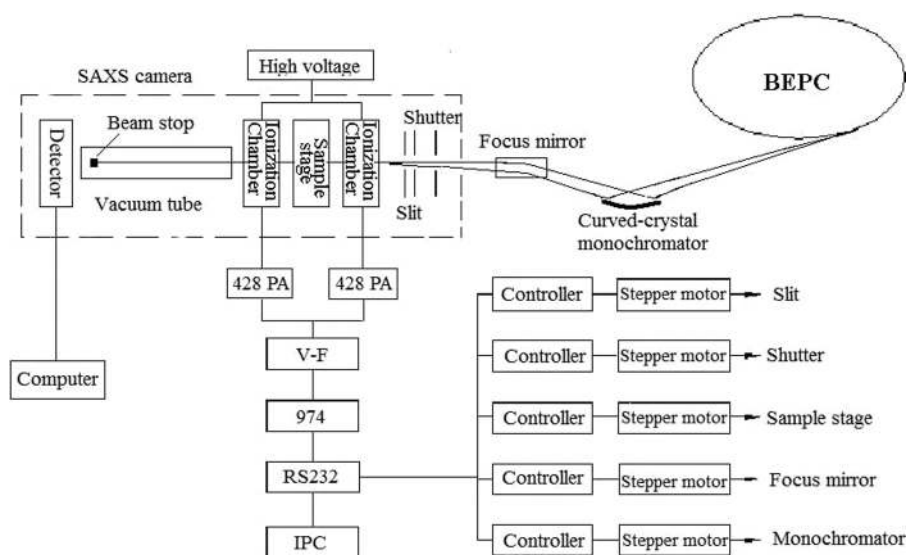


FIGURE 5 A schematic diagram of the computer-control system for the 1W2A small-angle X-ray scattering station.

behind the sample or by a photodiode from Forris Technologies embedded in the beamstop. The incident and transmitted X-ray intensities are used to normalize the small-angle X-ray scatterings intensity and the sample thickness. A schematic diagram of the computer-control system is shown in Figure 5.

A suite of software written with Intel Visual Fortran has been developed for small-angle X-ray scattering data processing and analysis.^[22] This software is composed of two modules. One is used for the primary data processing, such as the determination of the central position of the direct beam, the conversion of small-angle X-ray scattering pattern from pixel-space to q -space, the calibration of the scattering vector q , the correction of collimation error, the removal of the scattering background, and the normalization of the small-angle X-ray scattering intensity. Another is used for the data analysis, which includes Porod analysis, Debye analysis, Guinier approximation, shape evaluation, particle size distribution, and fractal analysis. In addition, both the de-smearred or slit-smearred small-angle X-ray scattering data can be processed in all the above data analysis, depending on the experimental condition.

APPLICATIONS

The 1W2A small-angle X-ray scattering station at Beijing Synchrotron Radiation Facility has steadily operated for more than five years. Although

the facility has only 2–3 months of dedicated beam-time supplied to users each year, the 1W2A small-angle X-ray scattering station still provides a superior site for users to do small-angle X-ray scattering studies. Due to the limited number of small-angle X-ray scattering stations in China, the 1W2A station has to frequently switch the experimental modes to satisfy different requirements from users. On the other hand, it also results in the research fields of the 1W2A experimental station covering multiple disciplines, such as biology, material chemistry, colloid chemistry, catalysis, nanomaterials, and polymers. Here, only representative experiments are briefly introduced to illustrate applications of the 1W2A small-angle X-ray scattering station at Beijing Synchrotron Radiation Facility.

Surfactants

Surfactants not only have the ability to self-assemble into morphologically different structures, such as micelles, vesicles, and liquid crystals, but also have wider applications in chemical engineering, material science, biology, environmental science, food industry, detergents, and enhanced oil recovery. Usually, surfactants can self-assemble into nanoscale structures, and hence the self-assembly structures of surfactants is an important application of small-angle X-ray scattering. Based on the experimental data collected at the 1W2A small-angle X-ray scattering station, combining with the electron microscopy observation, Zhang and Han^[9] studied a surfactant system of bisulfosuccinate sodium salt/water. A reversible switching of lamellar liquid crystals into micellar solutions induced by the compressed carbon dioxide was confirmed by the *in situ* small-angle X-ray scattering measurements. The reversible phase transition from lamellar liquid crystal (L_a) to micellar solution (L_1) can be well controlled by the CO_2 pressure at ambient temperature. This ambient-temperature transition is advantageous because of its simplicity and low-energy consumption. At the same time, this CO_2 -controlled phase transition between surfactant assemblies may have wider applications in material synthesis, polymerization, and chemical reactions.

Proteins

Most protein molecular sizes are in the nanoscale dimension, which implies that small-angle X-ray scattering technique is a suitable tool to elucidate protein molecular configuration. It is well known that the structural information of protein molecules and complexes is necessary to determine their biological function. However, it is very difficult to form crystals of some protein molecules. On the other hand, protein molecular configuration in

solution is better simulates to its real status in a physiological environment. Therefore, small-angle X-ray scattering is a preferential probe for the molecular shape and polymerization form of protein in solution. The protein elicitor from *Alternaria tenuissima* (PeaT1) presented excellent thermotolerance and potential application in agriculture as a pesticide. However, its thermotolerant mechanism was unclear. Xing et al.^[23] studied the shape evolution with temperature of the PeaT1 protein in solution by using small-angle X-ray scattering technique. They found that the PeaT1 protein molecules consisted of NAC, F, T, and UBA four structural domains, and formed a homodimeric structure in the solution. The shape change of the PeaT1 homodimer in solution is approximately reversible with temperature change. With increasing temperature, the two molecules in a PeaT1 homodimer are pushed away from each other. With decreasing temperature, the two molecules are attracted. During a heating-cooling cycle, the two NAC domains hugged each other face-to-face, and their relatively stable structure play a crucial role of frame in the thermotolerance of the PeaT1 protein. The PeaT1 protein presents a higher thermotolerance through the reversible structural relaxation.

Polymers

Polymers are one of the main research fields of the 1W2A small-angle X-ray scattering station at Beijing Synchrotron Radiation Facility. Many user researches focus on the crystallization behaviors of different polymer samples. For example, the crystallization behavior^[11] of a series of poly(ethylene-co-octene)s with different octene contents was studied under the shear stress by an *in situ* wide-angle X-ray diffraction and time-resolved small-angle X-ray scattering techniques. The results indicated that the initial states of the polymer melt play an important role in affecting the crystallization behaviors. The difference of the shear-induced crystalline structure evolution and the orientation between crystallite and lamellae supported the preordered mesomorphic phase of flexible polymer crystallization process proposed by Strobl.

Films

As excellent transparent conducting oxide films, sol-gel derived ITO films have wide applications in electric devices and thermal insulations fields such as liquid crystal display, solar cells, sensors, and heat-reflective windows glazing. Small-angle X-ray scattering, especially the grazing incidence small-angle X-ray scattering, is often used to probe the nanoscale structures in film materials. Yang et al. treated three thermal routes on

the sol-gel ITO films, i.e., conventional thermal annealing (CTA), rapid thermal annealing (RTA), and thermal cycle annealing (TCA). The near surface and internal structures of films were characterized by grazing incidence small-angle X-ray scattering at the 1W2A station.^[21] It was found that slit-like pores show fractal structures laterally and the near surface is sparser with bigger pores. Ordered pore structure normal to the film appeared when films were annealed at high heating rate. The shrinkage of pores was mainly due to structural relaxation and diffusion during the superheating process. However, the supercooling process has no significant effect on the structures. Furthermore, CTA samples have the greatest porosity and surface roughness due to the prevailing crystallization as well as the coarsening procedure. However small, pores inside the films are eliminated at low temperature.

Nanoparticles

It may be said that small-angle X-ray scattering is well designed to study the nanoscale structures in a material. Nanoparticles are especially appropriate to small-angle X-ray scattering research because of their nanoscale sizes. In addition, nanoparticles are also frequently the research object for individuals to seek after the nucleation mechanism and growth manner of materials. The use of the small-angle X-ray scattering technique to probe the nucleation and growth regularity of nanomaterials is an issue studied by current academic scientists. Wang et al.^[13] studied the size and shape evolution of gold nanoparticles in aqueous solution by using real-time small-angle X-ray scattering and ultraviolet-visible spectra at the 1W2A small-angle X-ray scattering station of Beijing synchrotron Radiation Facility. Gold nanoparticles were prepared by the seed mediated wet growth method. The size and shape evolution of both gold nanoparticles (nanospheres and nanorods) as well as their volume fractions were obtained. They found that a mutual competitive growth occurred between the gold nanorods and nanospheres within the first 18 min after adding the seed-solution into the growth solution to form a particle suspension. The average particle sizes always increased with growth time, but the evolution of size and shape of gold nanoparticles was almost stopped after 18 min. The aspect ratio of gold nanorods in the particle suspension was also obtained to follow an exponential decay change after the initial 5-min growth.

CONCLUSIONS

In summary, a versatile user-friendly small-angle X-ray scattering station has been constructed at Beijing Synchrotron Radiation Facility. The steady

operation of this station illustrates that it acclimatizes not only the dedicated mode but also the parasitic mode of Beijing Synchrotron Radiation Facility on the Beijing Electron Positron Collider. Besides routine small-angle X-ray scattering, combined small-angle and wide-angle X-ray scattering, grazing incidence small-angle X-ray scattering, and time-resolved scattering in millisecond level can be also performed at this station. In addition, multiple sample environments including temperature, stress-strain, and liquid sampling systems are available for *in situ* or real-time measurements. Since the 1W2A small-angle X-ray scattering station was commissioned in 2007, it has served successfully as the main facility of small-angle X-ray scattering study in China. It may be said that the 1W2A small-angle X-ray scattering station not only partially satisfies the user demand for small-angle X-ray scattering beam time, but also motivate users' research interests in China on small-angle X-ray scattering techniques. The 1W2A station plays an important role in fostering the user community of small-angle X-ray scattering in China, which will stimulate greatly the development of small-angle X-ray scattering techniques especially in the third-generation synchrotron radiation source of China. With the increase of user numbers and applications of small-angle X-ray scattering, the demand for better performance of small-angle X-ray scattering facility will further increase. Therefore, a further upgrade for the sample environmental system and the equipment of the 1W2A station is under consideration. We believe that the expert small-angle X-ray scattering stations with special design for respective discipline researches are a developing direction if the synchrotron radiation source has enough capacity for the beam lines.

ACKNOWLEDGMENT

We are grateful to Prof. Baozhong Dong (Beijing Synchrotron Radiation Facility, Beijing, China), Dr. Sérgio Funari (Hasylab at the Deutsches Elektronen-Synchrotron, Hamburg, Germany), and Dr. Michel Koch (European Molecular Biology Laboratory, Hamburg, Germany) for valuable discussion and advice. A part of this work was financially supported by the grants from the National Basic Research Program of China (2011CB911104) and the National Nature Science Foundation of China (Nos. U1332107, 11305198, U1232203, 111107903928, 21276278, 21176255, 10979005, 11079041).

REFERENCES

1. Glatter, O.; Kratky, O. *Small Angle X-ray Scattering*. Academic Press: New York, 1982.
2. Lightsources of the world: <http://www.lightsources.org/regions>, **2013**.

3. Institute of High Energy Physics, Chinese Academy of Sciences: <http://english.ihep.cas.cn/rs/fs/bepc/index.html>, **2013**.
4. Roessle, M. W.; Klaering, R.; Ristau, U.; Robrahn, B.; Jahn, D.; Gehrmann, T.; Konarev, P.; Round, A.; Fiedler, S.; Hermes, C.; Svergun, D. Upgrade of the small angle X-ray Scattering Beamline X33 at the European molecular biology laboratory, Hamburg. *J. Appl. Cryst.* **2007**, *40*, s190–s194.
5. Youli, L.; Roy, B.; Tuo, H.; Myung, C. C.; Morito, D. Scatterless hybrid metal–single-crystal slit for small angle X-ray scattering and high-resolution X-ray diffraction. *J. Appl. Cryst.* **2008**, *41*, 1134–1139.
6. The SX-165 Single Chip CCD Detector System: <http://www.marresearch.com/products.sx-165.html>, **2009**.
7. Shang, W.; Robrahn, B.; Golding, F.; Koch, M. H. J. A versatile data acquisition system for time resolved X-ray scattering using gas proportional detectors with delay line readout. *Nucl. Instr. Meth.* **2004**, *A530*, 513–520.
8. Technical Specification and Operating Procedure of PILATUS 1MF Detector System (V1.7), Dectris Company: Switzerland. 2012.
9. Zhang, J. L.; Han, B. X.; Li, W.; Zhao, Y. J.; Hou, M. Q. Reversible switching of lamellar liquid crystals into micellar solutions using CO₂. *Angew. Chem. Int. Ed.* **2008**, *47*, 10119–10123.
10. Wei, Y.; Zhang, H.; Gao, Z. Q.; Wang, W. J.; Shtykova, V. E.; Xu, J. H.; Quansheng Liu, Q. S.; Dong, Y. H. Crystal and solution structures of methyltransferase RsmH provide basis for methylation of C1402 in 16S rRNA. *J. Struct. Biol.* **2012**, *179*, 29–40.
11. Wen, H. Y.; Li, H.; Xu, S. Y.; Xiao, S. L.; Li, H. F.; Jiang, S. C.; An, L. J.; Wu, Z. H. Shear effects on crystallization behavior of poly(ethylene-co-octene) copolymers. *J. Polym. Res.* **2012**, *19*, 9801.
12. Chen, H. J.; Li, S. Y.; Liu, X. J.; Li, R. P.; Detlef, M. S.; Wu, Z. H.; Li, Z. H. Evaluation on pore structures of organosilicate thin films by grazing incidence small-angle X-ray scattering. *J. Phys. Chem. B* **2009**, *113*, 12623–12627.
13. Wang, W.; Zhang, K. H.; Cai, Q.; Mo, G.; Xing, X. Q.; Cheng, W. D.; Chen, Z. J.; Wu, Z. H. Real-time SAXS and ultraviolet-visible spectral studies on size and shape evolution of gold nanoparticles in aqueous solution. *Eur. Phys. J. B* **2010**, *76*, 301–307.
14. Li, Z. H.; Li, D. F.; Mo, G.; Wu, Z. H. SAXS/WAXS at BSRF, 2nd Cross-Strait Synchrotron Radiation Research Symposium Abstracts & Program Booklet, National Synchrotron Radiation Research Center (NSRRC), Taiwan, 2012.
15. Liu, G. M.; Zheng, L. H.; Zhang, X. Q.; Li, C. C.; Jiang, S. C.; Wang, D. J. Reversible lamellar thickening induced by crystal transition in poly (butylene succinate). *Macromolecules* **2012**, *45*, 5487–5493.
16. Cai, Q.; Wang, Q.; Wang, W.; Mo, G.; Zhang, K. H.; Cheng, W. D.; Xing, X. Q.; Chen, Z. J.; Wu, Z. H. A furnace to 1200 K for in situ heating X-ray diffraction, small angle X-ray scattering, and X-ray absorption fine structure experiments. *Rev. Sci. Instrum.* **2008**, *79*, 126101.
17. Zhang, K. H.; Wang, W.; Cheng, W. D.; Xing, X. Q.; Mo, G.; Quan, C.; Chen, Z. J.; Wu, Z. H. Temperature-induced interfacial change in Au@SiO₂ core–shell nanoparticles detected by extended X-ray absorption fine structure. *J. Phys. Chem. C* **2010**, *114*, 41–49.
18. Zhang, F. H.; Yang, L. L.; Ge, D. T. Multifractal formation studies of layer-by-layer deposited silver-containing indium tin oxide nanocomposite films by GISAXS. *Physica B Condens. Matt.* **2009**, *404*(14–15), 2008–2011.
19. Wang, X. D.; Chen, X.; Zhao, Y. R.; Yue, X.; Li, Q. H.; Li, Z. H. Nonaqueous lyotropic liquid-crystalline phases formed by Gemini surfactants in a protic ionic liquid. *Langmuir* **2012**, *28*, 2476–2484.
20. Wu, F. G.; Yu, J. H.; Sun, S. F.; Sun, H. Y.; Luo, J. J.; Yu, Z. W. Stepwise ordering of imidazolium-based cationic surfactants during cooling-induced crystallization. *Langmuir* **2012**, *28*, 7350–7359.
21. Yang, L. L.; He, X. D.; Ge, D. T.; Wei, H. Densification study of ITO films during high temperature annealing by GISAXS. *Physica B* **2009**, *404*, 2146–2150.
22. Li, Z. H. A program for SAXS data processing and analysis. *Chinese Phys. C* **2013**, *37*(10), 108002.
23. Xing, X. Q.; Liu, Q.; Wang, W.; Zhang, K. H.; Li, T.; Cai, Q.; Mo, G.; Cheng, W. D.; Wang, D. H.; Gong, Y.; Chen, Z. J.; Qiu, D. W.; Wu, Z. H. Shape evolution with temperature of a thermotolerant protein (PeaT1) in solution detected by small angle X-ray scattering. *Proteins* **2013**, *81*, 53–62.